surfaces

MDPI

Article

Electrophoretic Deposition of Hydroxyapatite–Chitosan–Titania on Stainless Steel 316 L

Leila Sorkhi [1,*], Morteza Farrokhi-Rad [2] and Taghi Shahrabi [3]

[1] Department of Materials and Metallurgical Engineering, South Dakota School of Mines and Technology, Rapid City, SD 57701, USA
[2] Department of Materials Engineering, Azarbaijan Shahid Madani University, 53751-71379 Tabriz, Iran
[3] Department of Materials Engineering, Faculty of Engineering, Tarbiat Modares University, P.O. Box 14115-143, Tehran, Iran
* Correspondence: Leila.sorkhi@mines.sdsmt.edu

Received: 13 June 2019; Accepted: 25 July 2019; Published: 29 July 2019

Abstract: In this research, hydroxyapatite (HA)–chitosan–titania nanocomposite coatings were formed on 316 L stainless steel using electrophoretic deposition (EPD) from alcoholic (methanol and ethanol) suspensions containing 0.5 g/L chitosan and 2 and 5 g/L HA and 2 and 5 g/L Titania. The effect of different parameters on the deposition rate, morphology, and corrosion resistance of the coatings in simulated body fluid (SBF) at 37 °C has been studied. The coatings' properties were investigated using Fourier-transform infrared spectroscopy (FTIR) and scanning electron microscope (SEM). Based on the results of this work, it was found that the deposition rate in ethanolic suspensions is lower than methanolic ones. Moreover, the coating surface was smoother when the ethanol was used as a solvent in suspensions in comparison to the ones where methanol was the solvent. The coating deposited from a suspension containing 0.5 g/L chitosan, 2 g/L HA, and 5 g/L titania with ethanol as solvent had the highest corrosion resistance in SBF at 37 °C.

Keywords: electrophoretic deposition; nanocomposite; chitosan; hydroxyapatite; titania

1. Introduction

Hydroxyapatite $Ca_{10}(PO_4)_6(OH)_2$ (HA) is a crystalline material that has been used as a coating for metallic body implants because of its biocompatibility, bioactivity, and similarity to the chemical composition of the inorganic part of bone tissue [1–6]. In terms of coating, there are several methods to form HA, including sol-gel [7], plasma spraying [5,8], and electrochemical deposition [9]. Among all different methods, electrophoretic deposition (EPD) is one of the most promising methods to produce HA coatings. This method is a very simple and flexible method that can be applied to any complex shaped material leading to the formation of the uniform coating. In comparison to the other methods, EPD has the superiority of being less time-consuming and less expensive. This colloidal process works such that charged particles in a liquid medium immigrate due to the influence of an electrical potential gradient, so their coagulation on an electrode with opposite charge forms a deposit [1,3,6,10–14].

The weight of the coatings fabricated by EPD process can be represented by Hamaker Equation (1), where C and μ are concentration and electrophoretic mobility of particles in the suspension, t and A are deposition time and area, and E is the applied electric field [15].

$$W = C.\mu.A.E.t, \quad (1)$$

HA coatings deposited by EPD usually need a further sintering process at a relatively high temperature to resolve some of its defects, such as low fracture toughness, high brittleness, and weak

bonding to the substrate. Oxidation of substrate and thermal stresses in the coating and thermal decomposition of HA are the consequences of sintering [16–18]. Problems caused by sintering could be mitigated by adding polymer to HA coatings [1]. Chitosan is a linear cationic polysaccharide consisting of β (1→4)-glucosamine and *N*-acetyl-D-glucosamine, which can be produced by alkaline N-deacetylation of chitin.

In biomedical science, chitosan has many applications, including drug encapsulation and tissue engineering scaffolds. It has also been applied as a coating material for surface modification of orthopedic implants because of its similarity to the extracellular matrix of bone and cartilage and unique physicochemical properties, like biocompatibility, non-toxicity, biodegradability, biofunctionality, antibacterial activity, and chemical resistance [1,2,13,18–21]. In the acidic medium, chitosan becomes a positively charged polyelectrolyte as a result of the protonation of amino groups [22,23]. It has been reported that adding a small amount of citric acid to the HA–chitosan suspensions improves the mechanical properties of coating, such as Young's modulus and compression strength, and increases the size of HA-chitosan precipitated on the substrate [24]. Fabrication of HA–chitosan coatings have been investigated using various methods [18,25–27]. Feasibility of producing HA–chitosan coating from alcoholic suspensions using EPD method on metallic substrates has been demonstrated [1,28].

Titania has been used extensively in biomaterial applications due to its excellent biocompatibility and good corrosion resistance. Furthermore, the addition of titania nanoparticles to the HA coatings enhances the mechanical properties and therefore stability of coating [29,30]. Titania–HA bilayer coatings have more corrosion resistance and adhesion strength to the titanium (Ti) substrate in comparison to HA coatings fabricated by EPD [31,32]. Bioactivity and adherence of HA coatings to the implant can be ameliorated by adding bioactive titania powders [32]. Farnoush et al. [33] reported enhancement of adhesion strength and fracture toughness and decrease of corrosion rate of coatings in SBF by the implementation of titania to the HA coatings on the Ti–6Al–4V substrate [34]. EPD process has been used to produce HA + titania nanocomposite on Ti alloy, which is a hard coating with high wear and corrosion resistance [30,33–35]. Mohan et al. [35] determined that the strength and adherence of the coating to the substrate increased by sintering, whereas the corrosion resistance was decreased. Nathanael et al. [36] reported an increase in mechanical strength of HA–titania nanocoating fabricated by the sol-gel method compared to HA coatings. Kavitha et al. [37] fabricated chitosan titania nanocomposites using in vitro sol-gel method. Synthesized coatings showed high surface area, appropriate HA formation, and specific antibacterial action, which reveals the application of titania–chitosan nanocomposites for orthopedic and tissue engineering.

To the best of the author's knowledge, fabrication of HA–chitosan–titania coatings using EPD has not been reported. In this study, HA–chitosan–titania nanocomposite coatings with various amounts of HA and titania were electrophoretically deposited. The fabricated coatings were characterized by employing SEM. Finally, the coatings' corrosion resistance in SBF was studied.

2. Materials and Methods

2.1. Suspensions Preparation

In this work, the wet chemical method was used to synthesize HA nanoparticles [27]. Obtained spherical HA nanoparticles with a diameter of about 20–30 nm were used in order to prepare the suspensions. Chitosan (MW = 300 kDa, degree of deacetylation of about 85%), acetic acid (99.8%), and titania (21 nm) were respectively purchased from Acros Organics (Geel, Belgium), Merck (Kenilworth, NJ, USA), and Degussa (Frankfurt, Germany) and used for suspension preparation. The deposition was accomplished using the 0.5 g/L chitosan suspensions containing HA and titania nanoparticles in the mixture of alcohol and water (ethanol with 15% distilled water or methanol with 5% distilled water) containing 0.05 vol % acetic acid. The latter was added to the suspensions to propagate the dissolution of chitosan. All suspensions were magnetically stirred for 5 h followed

by 10 min ultrasonication (Bandelin, Berlin, Germany, Sonopuls HD 3200, 20 kHz) to break down the agglomerates.

2.2. Electrophoretic Deposition

A two-electrode cell was applied to perform the EPD. Both substrates and counter electrode were 10 mm × 20 mm × 1 mm pieces of 316 L stainless steel. Only 1 cm^2 of each plate exposed to the suspension and the remainder area was insulated, and the distance between the two electrodes in the cell was 1 cm. EPD was accomplished at 20 V/cm and for various times (0.5, 2, 4, 6, 8, and 10 min). To record the current density during EPD, a computer-connected digital multimeter (Fluke, Everett, WA, USA, 289 True RMS) was used. In order to calculate the weight of the coatings, the weight of the samples was measured after overnight drying in air and deducted by the weight of them before deposition using a digital scale with 0.1 mg accuracy (Sartorius, Göttingen, Germany, CP324s). The microstructure of the coatings deposited at 20 V/cm from the various alcoholic suspensions with the various concentrations of titania and HA nanoparticles (2 and 5 g/L was observed by a scanning electron microscope (SEM) (Electron Optic Services, Ottawa, ON, Canada).

2.3. Corrosion Resistance

Potentiodynamic polarization tests were carried out using a potentiostat/galvanostat (Autolab, Utrecht, The Netherlands) in a standard three electrode electrochemical cell with a platinum plate as the counter electrode, and a saturated calomel electrode as the reference electrode (scan rate: 1 mV/s, scan range E_{ocp} − 0.2 to E_{ocp} + 0.8) was used to study the polarization corrosion behavior of the stainless steel 316 L coated with HA–chitosan–titania nanocomposite as well as the bare metal in SBF at 37 °C [38].

3. Results and Discussion

3.1. Current Density

Figure 1 depicts the current density measured by multimeter during the EPD process at 20 V/cm, from ethanolic and methanolic suspensions containing 0.5 g/L chitosan and various concentrations of HA and titania. Usually, during the EPD process, an insulating ceramic layer is formed on the substrate electrode, which results in the descending trend of the current density. The relatively constant trend of current densities here is because of the existence of water molecules in the suspensions and electrolysis of water on the substrate electrode, which results in the low electrical resistance of the deposits. Due to the higher electrical conductivity of methanolic suspensions, current densities passing through the EPD circuit for methanolic suspensions are higher than ethanolic suspensions.

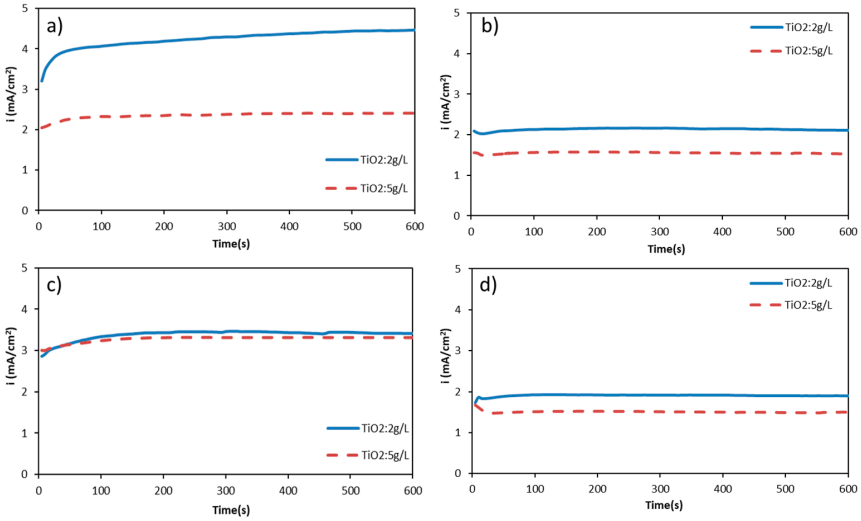

Figure 1. Current density variations during electrophoretic deposition (EPD) process from alcoholic suspensions (**a**,**c**) methanol and (**b**,**d**) ethanol, containing 0.5 g/L chitosan 2 (**a**,**b**) and 5 (**c**,**d**) g/L hydroxyapatite (HA) with various concentration of titania at 20 V/cm.

3.2. Kinetics of Deposition

The weight of coatings deposited from different alcoholic suspensions (methanol and ethanol) containing 0.5 g/L chitosan, 0.05 vol % acetic acid, various concentrations of HA and titania nanoparticles (2 and 5 g/L) is depicted as a function of time in Figure 2. It illustrates that the deposition weight increases with time in a linear trend that can be demonstrated by the Hamaker equation, and the slope of this line indicates the rate of deposition. As can be explained by the Hamaker Equation (1), the deposition rate increases by increasing the concentration of HA or titania nanoparticles. Higher deposition weight of coating from methanolic suspensions is because of higher electrophoretic mobility of particles in the alcohol with lower molecular weight.

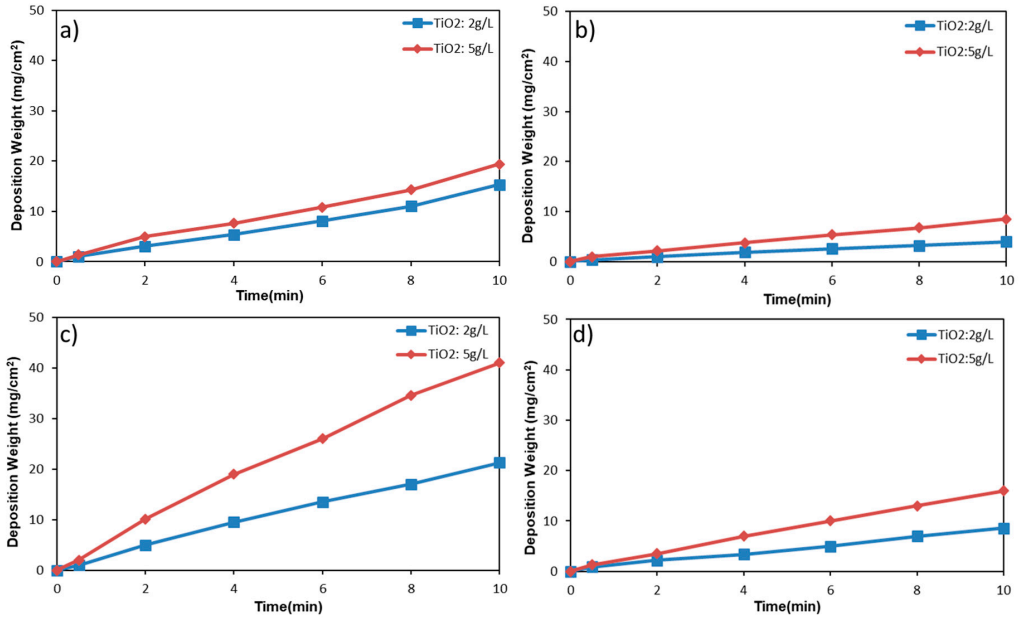

Figure 2. Weight of HA–chitosan–titania coatings deposited at 20 V/cm, from alcoholic suspensions (**a**,**c**) methanol and (**b**,**d**) ethanol, containing 0.5 g/L chitosan, 2 (**a**,**b**) and 5 (**c**,**d**) HA and 2 and 5 g/L titania.

3.3. FTIR Analysis

The result of FTIR analysis of coating separated from the substrate is represented in Figure 3. This spectrum shows peaks at 636 and 3580 cm^{-1}, which are related to hydroxyl stretching vibration. The peaks correlated to the phosphate groups of HA are present at 536 and 963 cm^{-1}. The peak at 1421 cm^{-1} is attributed to the carbonate bonds. Apart from the peaks attributed to the HA, other peaks also appear in the FTIR analysis curve of the coating. The peak at 1595 cm^{-1} is related to the NH-bonding vibrations in the amide group of chitosan. The peaks at 1091 and 1654 cm^{-1} can be respectively attributed to the stretch of C–O bond in polysaccharide and stretching of C=O bond in amide I in chitosan. The presence of peaks related to chitosan proves the adsorption of chitosan on the HA nanoparticles. Moreover, there are peaks at 1825, 3580, and 3736 cm^{-1} that can be attributed to hydroxyl groups attached to titania. The peak at 760 cm^{-1} can be related to the vibration of the Ti–O bond. Presence of these peaks demonstrates the presence of titania in the coating.

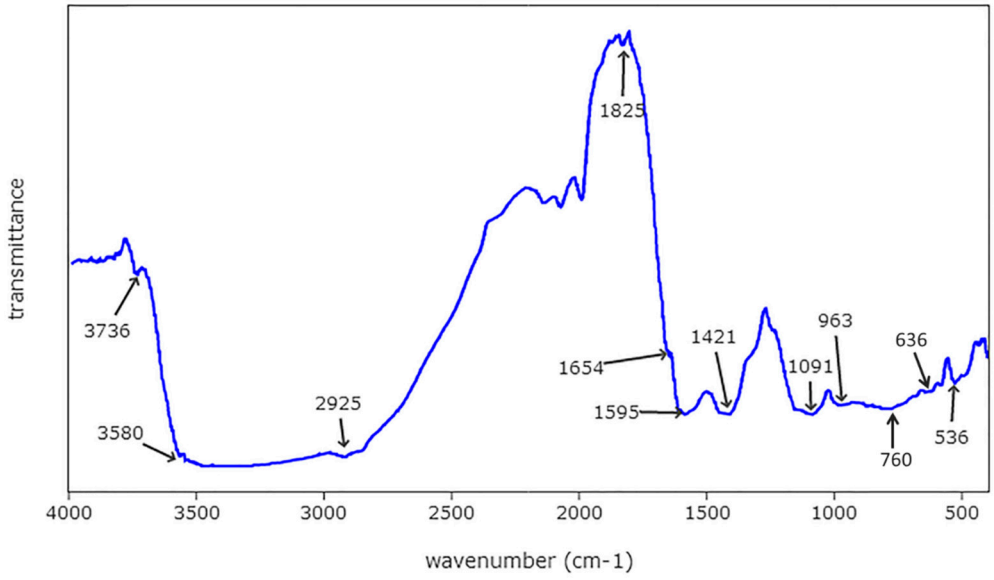

Figure 3. FTIR analysis for powders separated from various ethanolic suspension containing 0.5 g/L chitosan, 5 g/L HA, and 2 g/L titania.

3.4. SEM Analysis

Figure 4 shows SEM images of coatings deposited at 20 V/cm from 0.5 g/L chitosan suspensions containing 5 g/L HA and 2 g/L titania nanoparticles in methanol and ethanol. It can be inferred from Figure 4 that by increasing the ratio of titania to HA, the surface of the coating becomes smoother due to the smaller size of titania nanoparticles in comparison to HA nanoparticles. On the other hand, increasing the concentration of titania results in the cracking of the coatings, which is due to decrease of the ratio of chitosan to nanoparticles and the smaller size of titania nanoparticles in comparison to HA nanoparticles, as they adsorb more alcohol, resulting in an increase of shrinkage and cracking during the drying process.

Figure 5a,b shows higher magnification of Figure 4e,f, respectively. Comparing Figure 5a,b, the coating deposited from a suspension that contains ethanol as the solvent is smoother than the one with methanol as solvent. The reason is that in methanolic suspension, adsorption of chitosan on the HA nanoparticles is lower than ethanolic suspension, and therefore methanolic suspension has more agglomeration of HA nanoparticles [26].

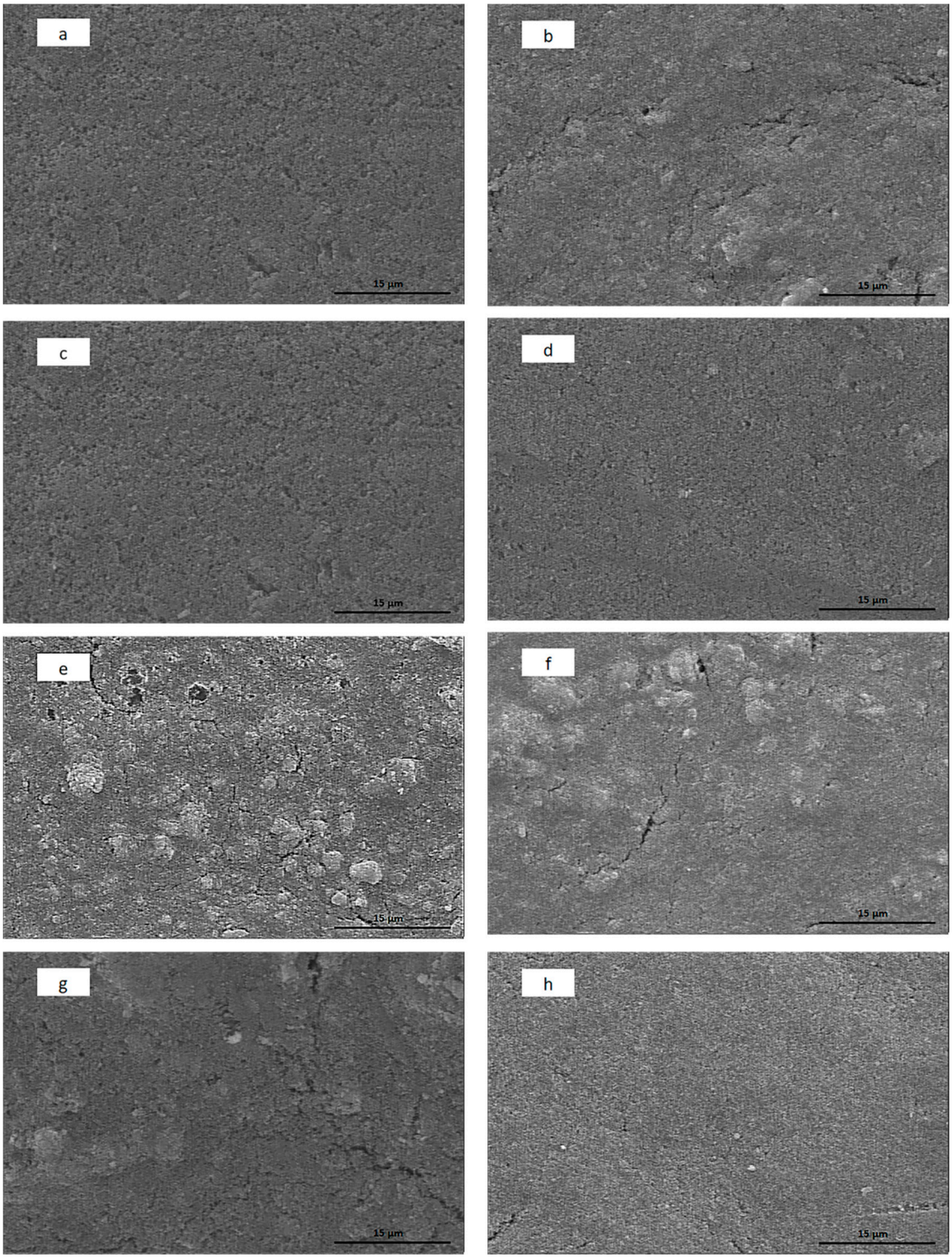

Figure 4. SEM images of coating deposited from methanolic (**a**,**c**,**e**,**g**) and ethanolic (**b**,**d**,**f**,**h**) suspensions containing 0.5 g/L chitosan, 2 (**a**,**b**,**c**,**d**) and 5 (**e**,**f**,**g**,**h**) g/L HA, and 2 (**a**,**b**,**e**,**f**) and 5 (**c**,**d**,**g**,**h**) g/L H titania at 20 V/cm.

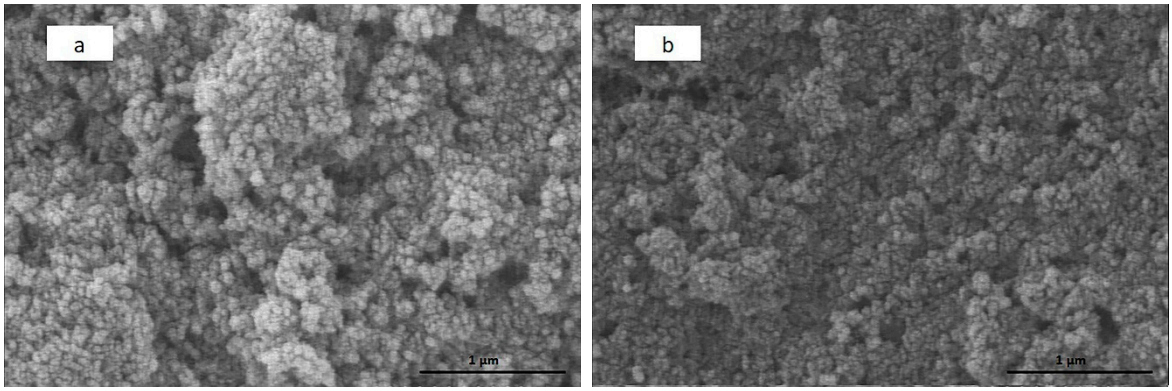

Figure 5. SEM images of coating deposited at 20 V/cm from methanolic (**a**) and ethanolic (**b**) suspensions containing 0.5 g/L chitosan 5 g/L HA and 2 g/L H titania.

3.5. Corrosion Resistance

Corrosion behavior of the coatings deposited at 20 V/cm and 30 s from suspensions containing 0.5 g/L chitosan, 2 and 5 g/L HA nanoparticles, and 2 and 5 g/L titania on SS 316 L substrate, as well as the uncoated substrate, was studied in SBF at 37 °C, and the polarization curves are depicted in Figure 6. The values of I_{corr} and E_{corr} are calculated using Tafel extrapolation and are listed in Table 1. It demonstrates that the corrosion resistance is increased as a result of the formation of coatings. Increasing the ratio of titania to HA also increases the corrosion resistivity, due to the smaller size of the titania particles which can fill the gaps between HA particles, preventing the development of crack. Furthermore, deposition rate in methanolic suspensions is higher compared to ethanolic ones, which in low solid concentration resulted in higher corrosion resistivity due to a higher thickness of coatings. Although in high solid concentration, coatings deposited from ethanolic suspensions have higher corrosion resistance due to the smoother surface.

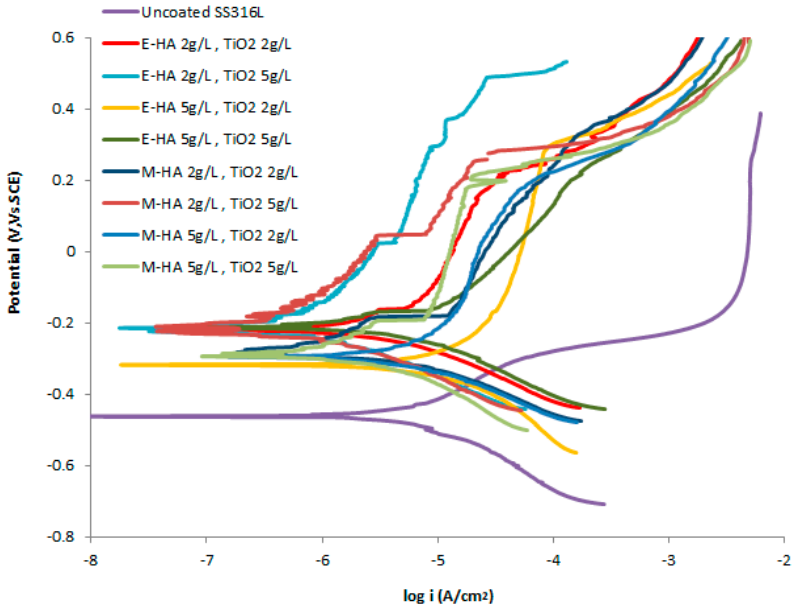

Figure 6. Corrosion behavior of uncoated 316 L stainless steel and coatings deposited at 20 V/cm and 30 s from methanolic and ethanolic suspensions containing 0.5 g/L chitosan, 2 and 5 g/L HA nanoparticles, and 2 and 5 g/L titania in SBF and at 37 °C.

Table 1. Corrosion current density (I_{corr}) and potential (E_{corr}) for bare stainless steel 316 L and coatings deposited at 20 V/cm and 30 s from methanolic and ethanolic suspensions containing 0.5 g/L chitosan, 2 and 5 g/L HA nanoparticles, and 2 and 5 g/L HA nanoparticles in SBF and at 37 °C.

Suspension for Coating	Icorr (A/cm^2)	Ecorr vs. SCE (V)
Uncoated Stainless steel 316 L	1.86×10^{-6}	−0.46
Ethanol—0.5 g/L Chitosan, HA 2 g/L and Titania 2 g/L	2.51×10^{-7}	−0.23
Ethanol—0.5 g/L Chitosan, HA 2 g/L and Titania 5 g/L	9.33×10^{-8}	−0.22
Ethanol—0.5 g/L Chitosan, HA 5 g/L and Titania 2 g/L	1.41×10^{-6}	−0.32
Ethanol—0.5 g/L Chitosan, HA 5 g/L and Titania 5 g/L	5.01×10^{-7}	−0.23
Methanol—0.5 g/L Chitosan, HA 2 g/L and Titania 2 g/L	3.16×10^{-7}	−0.27
Methanol—0.5 g/L Chitosan, HA 2 g/L and Titania 5 g/L	6.31×10^{-8}	−0.22
Methanol—0.5 g/L Chitosan, HA 5 g/L and Titania 2 g/L	1.10×10^{-6}	−0.29
Methanol—0.5 g/L Chitosan, HA 5 g/L and Titania 5 g/L	2.51×10^{-7}	−0.28

4. Conclusions

In this work, the HA–chitosan–titania nanocomposite coatings were deposited on 316 L stainless steel from ethanolic and methanolic suspensions using EPD technique. The weight of coatings increased linearly with time of deposition because of the presence of water in the suspensions, which increased the electrical conductivity of the deposited film. Because of the higher mobility of particles in lower weight alcohols, the weight of coatings was higher in the coatings deposited from suspensions that have methanol as solvent. FTIR analysis spectrum revealed peaks contributed to HA, chitosan, and titania and demonstrated their existence in the coating separated from the substrate. Increasing the ratio of titania to HA results in smoother coatings, although a higher concentration of titania results in cracking. At low concentration of solids (HA and titania), methanolic coatings have better corrosion resistance as a result of higher thickness, but higher solid concentration resulted in cracks and rough surface, hence lower corrosion resistance. The best coating surface quality and highest corrosion resistance were achieved by deposition from an ethanolic suspension containing 0.5 g/L chitosan, 2 g/L HA, and 5 g/L titania.

Author Contributions: Conceptualization, methodology, formal analysis, investigation, and writing: L.S.; conceptualization, methodology, and formal analysis: M.F.-R.; supervision and funding: T.S.

Funding: This research received no external funding

Conflicts of Interest: The authors declare no conflict of interest.

References

1. Pang, X.; Zhitomirsky, I. Electrophoretic deposition of composite hydroxyapatite-chitosan coatings. *Mater. Charact.* **2007**, *58*, 339–348. [CrossRef]
2. Moskalewicz, T.; Kot, M.; Seuss, S.; Kędzierska, A.; Czyrska-Filemonowicz, A.; Boccaccini, A.R. Electrophoretic deposition and characterization of HA/chitosan nanocomposite coatings on Ti6Al7Nb alloy. *Met. Mater. Int.* **2015**, *21*, 96–103. [CrossRef]
3. Rojaee, R.; Fathi, M.; Raeissi, K. Electrophoretic deposition of nanostructured hydroxyapatite coating on AZ91 magnesium, alloy implants with different surface treatments. *Appl. Surf. Sci.* **2013**, *285*, 664–673. [CrossRef]
4. Levingstone, T.J.; Ardhaoui, M.; Benyounis, K.; Looney, L.; Stokes, J.T. Plasma sprayed hydroxyapatite coatings: Understanding process relationships using design of experiment analysis. *Surf. Coat. Techol.* **2015**, *283*, 29–36. [CrossRef]
5. Yousefpour, M.; Afshar, A.; Chen, J.; Zhang, X. Electrophoretic deposition of porous hydroxyapatite coatings using polytetrafluoroethylene particles as templates. *Mater. Sci. Eng. C* **2007**, *27*, 1482–1486. [CrossRef]

6. Eliaz, N.S.T.M.; Sridhar, T.M.; Kamachi Mudali, U.; Raj, B. Electrochemical and electrophoretic deposition of hydroxyapatite for orthopaedic applications. *Surf. Eng.* **2005**, *21*, 238–242. [CrossRef]
7. Sidane, D.; Chicot, D.; Yala, S.; Ziani, S.; Khireddine, H.; Iost, A.; Decoopman, X. Study of the mechanical behavior and corrosion resistance of hydroxyapatite sol–gel thin coatings on 316 L stainless steel pre-coated with titania film. *Thin Solid Films* **2015**, *593*, 71–80. [CrossRef]
8. Demnati, I.; Parco, M.; Grossin, D.; Fagoaga, I.; Drouet, C.; Barykin, G.; Combes, C.; Braceras, I.; Gonçalvès, S.; Rey, C. Hydroxyapatite coating on titanium by a low energy plasma spraying mini-gun. *Surf. Coat. Technol.* **2012**, *206*, 2346–2353. [CrossRef]
9. He, D.H.; Wang, P.; Liu, P.; Liu, X.K.; Ma, F.C.; Zhao, J. HA coating fabricated by electrochemical deposition on modified Ti6Al4V alloy. *Surf. Coat. Technol.* **2016**, *301*, 6–12. [CrossRef]
10. Besra, L.; Liu, M. A review on fundamentals and applications of electrophoretic deposition (EPD). *Prog. Mater. Sci.* **2007**, *52*, 1–61. [CrossRef]
11. Farnoush, H.; Aldıç, G.; Çimenoğlu, H. Functionally graded HA–TiO_2 nanostructured composite coating on Ti–6Al–4V substrate via electrophoretic deposition. *Surf. Coat. Technol.* **2015**, *265*, 7–15. [CrossRef]
12. Corni, I.; Ryan, M.P.; Boccaccini, A.R. Electrophoretic deposition: From traditional ceramics to nanotechnology. *J. Eur. Ceram. Soc.* **2008**, *28*, 1353–1367. [CrossRef]
13. Molaei, A.; Yousefpour, M. Electrophoretic deposition of chitosan–bioglass®–hydroxyapatite–halloysite nanotube composite coating. *Rare Met.* **2018**, 1–8. [CrossRef]
14. Mishyn, V.; Aspermair, P.; Leroux, Y.; Happy, H.; Knoll, W.; Boukherroub, R.; Szunerits, S. "Click" Chemistry on Gold Electrodes Modified with Reduced Graphene Oxide by Electrophoretic Deposition. *Surfaces* **2019**, *2*, 193–204. [CrossRef]
15. Hamaker, H.C. Formation of a deposit by electrophoresis. *Trans. Faraday Soc.* **1940**, *35*, 279–287. [CrossRef]
16. Javidi, M.; Javadpour, S.; Bahrololoom, M.E.; Ma, J. Electrophoretic deposition of natural hydroxyapatite on medical grade 316L stainless steel. *Mater. Sci. Eng. C* **2008**, *28*, 1509–1515. [CrossRef]
17. Tang, S.; Tian, B.; Guo, Y.J.; Zhu, Z.A.; Guo, Y.P. Chitosan/carbonated hydroxyapatite composite coatings: Fabrication, structure and biocompatibility. *Surf. Coat. Technol.* **2014**, *251*, 210–216. [CrossRef]
18. Boccaccini, A.R.; Keim, S.; Ma, R.; Li, Y.; Zhitomirsky, I. Electrophoretic deposition of biomaterials. *J. R. Soc. Interface* **2010**, *7*, S581–S613. [CrossRef]
19. Ma, R.; Zhitomirsky, I. Electrophoretic deposition of chitosan–albumin and alginate–albumin films. *Surf. Eng.* **2011**, *27*, 51–56. [CrossRef]
20. Pishbin, F.; Simchi, A.; Ryan, M.P.; Boccaccini, A.R. Electrophoretic deposition of chitosan/45S5 Bioglass® composite coatings for orthopaedic applications. *Surf. Coat. Technol.* **2011**, *205*, 5260–5268. [CrossRef]
21. Đošić, M.; Eraković, S.; Janković, A.; Vukašinović-Sekulić, M.; Matić, I.Z.; Stojanović, J.; Rhee, K.Y.; Mišković-Stanković, V.; Park, S.J. In vitro investigation of electrophoretically deposited bioactive hydroxyapatite/chitosan coatings reinforced by graphene. *J. Ind. Eng. Chem.* **2017**, *47*, 336–347. [CrossRef]
22. Pang, X.; Zhitomirsky, I. Electrodeposition of composite hydroxyapatite–chitosan films. *Mater. Chem. Phys.* **2005**, *94*, 245–251. [CrossRef]
23. Sorkhi, L.; Farrokhi-Rad, M.; Shahrabi, T. Electrophoretic deposition of chitosan in different alcohols. *J. Coat. Technol. Res.* **2014**, *11*, 739–746. [CrossRef]
24. Yamaguchi, I.; Iizuka, S.; Osaka, A.; Monma, H.; Tanaka, J. The effect of citric acid addition on chitosan/hydroxyapatite composites. *Colloids Surf. A* **2003**, *214*, 111–118. [CrossRef]
25. Heidari, F.; Bahrololoom, M.E.; Vashaee, D.; Tayebi, L. In situ preparation of iron oxide nanoparticles in natural hydroxyapatite/chitosan matrix for bone tissue engineering application. *Ceram. Int.* **2015**, *41*, 3094–3100. [CrossRef]
26. Song, L.; Gan, L.; Xiao, Y.F.; Wu, Y.; Wu, F.; Gu, Z.W. Antibacterial hydroxyapatite/chitosan complex coatings with superior osteoblastic cell response. *Mater. Lett.* **2011**, *65*, 974–977. [CrossRef]
27. Hahn, B.D.; Park, D.S.; Choi, J.J.; Ryu, J.; Yoon, W.H.; Choi, J.H.; Kim, H.E.; Kim, S.G. Aerosol deposition of hydroxyapatite–chitosan composite coatings on biodegradable magnesium alloy. *Surf. Coat. Technol.* **2011**, *205*, 3112–3118. [CrossRef]
28. Mahmoodi, S.; Sorkhi, L.; Farrokhi-Rad, M.; Shahrabi, T. Electrophoretic deposition of hydroxyapatite–chitosan nanocomposite coatings in different alcohols. *Surf. Coat. Technol.* **2013**, *216*, 106–114. [CrossRef]
29. Sarkar, A.; Kannan, S. In situ synthesis, fabrication and Rietveld refinement of the hydroxyapatite/titania composite coatings on 316 L SS. *Ceram. Int.* **2014**, *40*, 6453–6463. [CrossRef]

30. Lee, C.K. Fabrication, characterization and wear corrosion testing of bioactive hydroxyapatite/nano-TiO_2 composite coatings on anodic Ti–6Al–4V substrate for biomedical applications. *Mater. Sci. Eng. B* **2012**, *177*, 810–818. [CrossRef]
31. Rath, P.C.; Besra, L.; Singh, B.P.; Bhattacharjee, S. Titania/hydroxyapatite bi-layer coating on Ti metal by electrophoretic deposition: Characterization and corrosion studies. *Ceram. Int.* **2012**, *38*, 3209–3216. [CrossRef]
32. Albayrak, O.; El-Atwani, O.; Altintas, S. Hydroxyapatite coating on titanium substrate by electrophoretic deposition method: Effects of titanium dioxide inner layer on adhesion strength and hydroxyapatite decomposition. *Surf. Coat. Technol.* **2008**, *202*, 2482–2487. [CrossRef]
33. Farnoush, H.; Mohandesi, J.A.; Çimenoğlu, H. Micro-scratch and corrosion behavior of functionally graded HA-TiO2 nanostructured composite coatings fabricated by electrophoretic deposition. *J. Mech. Behav. Biomed. Mater.* **2015**, *46*, 31–40. [CrossRef]
34. Farnoush, H.; Mohandesi, J.A.; Fatmehsari, D.H.; Moztarzadeh, F. A kinetic study on the electrophoretic deposition of hydroxyapatite–titania nanocomposite based on a statistical approach. *Ceram. Int.* **2012**, *38*, 6753–6767. [CrossRef]
35. Mohan, L.; Durgalakshmi, D.; Geetha, M.; Narayanan, T.S.; Asokamani, R. Electrophoretic deposition of nanocomposite (HAp+ TiO_2) on titanium alloy for biomedical applications. *Ceram. Int.* **2012**, *38*, 3435–3443. [CrossRef]
36. Nathanael, A.J.; Mangalaraj, D.; Ponpandian, N. Controlled growth and investigations on the morphology and mechanical properties of hydroxyapatite/titania nanocomposite thin films. *Compos. Sci. Technol.* **2010**, *70*, 1645–1651. [CrossRef]
37. Kavitha, K.; Sutha, S.; Prabhu, M.; Rajendran, V.; Jayakumar, T. In situ synthesized novel biocompatible titania–chitosan nanocomposites with high surface area and antibacterial activity. *Carbohydr. Polym.* **2013**, *93*, 731–739. [CrossRef]
38. Kokubo, T.; Takadama, H. How useful is SBF in predicting in vivo bone bioactivity? *Biomaterials* **2006**, *27*, 2907–2915. [CrossRef]